



Anisotropy of Interfaces in an Ordered HCP Binary Alloy

J. W. Cahn¹
S. C. Han²
G. B. McFadden¹

¹U.S. DEPARTMENT OF COMMERCE
Technology Administration
National Institute of Standards
and Technology
Gaithersburg, MD 20899-0001

²Montgomery Blair High School
Silver Spring, MD 20910-5569

QC
100
.U56
NO.6217
1998

Anisotropy of Interfaces in an Ordered HCP Binary Alloy

J. W. Cahn¹
S. C. Han²
G. B. McFadden¹

¹U.S. DEPARTMENT OF COMMERCE
Technology Administration
National Institute of Standards
and Technology
Gaithersburg, MD 20899-0001

²Montgomery Blair High School
Silver Spring, MD 20910-5569

September 1998



U.S. DEPARTMENT OF COMMERCE
William M. Daley, Secretary

TECHNOLOGY ADMINISTRATION
Gary R. Bachula, Acting Under Secretary
for Technology

NATIONAL INSTITUTE OF STANDARDS
AND TECHNOLOGY
Raymond G. Kammer, Director

Anisotropy of Interfaces in an Ordered HCP Binary Alloy

J.W. Cahn¹, S.C. Han^{2,*}, and G.B. McFadden^{1,†}

¹National Institute of Standards and Technology

Gaithersburg, MD 20899, USA

²Montgomery Blair High School

Silver Spring, MD 20910-5569, USA

Abstract

A multiple-order-parameter mean field theory of ordering on a binary hexagonal-close-packed (HCP) crystal structure is developed, and adapted to provide a continuum formulation that incorporates the underlying symmetries of the HCP crystal in both the bulk and gradient energy terms of the free energy. The work is an extension of the previous treatment by Braun et al. [Phil. Trans. Roy. Soc. Lond. A 355 (1997), p. 1787] of order-disorder transitions on a face-centered-cubic crystal (FCC) lattice. The theory is used to compute the orientation dependence of the structure and energy of interphase and antiphase boundaries in ordering to the Cd₃Mg and CdMg structures, which are the HCP analogs of Cu₃Au and CuAu structures in FCC. As in the corresponding FCC case, the multiple order parameters do not form a vector. Anisotropy is a natural consequence of the underlying crystal symmetries and the multiple-order-parameter continuum formation presented here. The isotropy transverse to the six-fold axis expected for a scalar order parameter is not found.

Key Words: Diffuse interfaces; hexagonal close packing; anisotropy; mean field theory; Allen-Cahn equation; interphase boundaries; antiphase boundaries; surface energy; discrete free energy.

*Current address: Yale University, New Haven, CT 06520

†Corresponding author: mcfadden@nist.gov

1 Introduction

Continuum diffuse interface theories of solid-state phase equilibria are based on thermodynamic descriptions in which the conventional free energy densities for the bulk phases are augmented by gradient energy terms whose specific forms reflect the underlying symmetries of the crystal [1]. For example, in the mean-field description of order-disorder transitions of a binary FCC crystal considered by Braun et al. [2,3] three nonconserved order parameters X_j are used to model the disordered phase and the ordered phases AB_3 and A_2B_2 . The gradient energy term is a quadratic form in the spatial gradients $\partial X_j / \partial x_k = X_{j,k}$ having the general form $c_{jklm} X_{j,k} X_{l,m}$, where the coefficients c_{jklm} reflect the FCC crystal symmetry. Surprisingly, Braun et al. find that the resulting symmetry of the coefficients c_{jklm} is not that of a general fourth rank tensor for a cubic material [4], which is a consequence of the fact that the nonconserved order parameters X_j do not transform as a tensor under the appropriate changes in coordinates. Braun et al. determined the form of the coefficients in two equivalent ways, first by invoking invariance of the gradient energy term to symmetry operations, and also by evaluating the gradient energy terms in a continuum limit of a discrete Ising-type model that takes into account nearest and second nearest neighbor interactions.

In this paper we consider the analogous form of the gradient energy term for an hexagonal close packed (HCP) binary alloy, by considering the continuum limit of a discrete Ising-like model. In an appropriate coordinate system, both the HCP and FCC structures can be described in terms of the layering of close-packed planes. Neighboring planes are shifted relative to one another, with the HCP structure described by alternating stacking of two layers [a-b-a-b] and a space group symmetry $P6_3mmc$, whereas the FCC structure involves the stacking of three such shifted layers [a-b-c-a-b-c], and a loss of the six-fold symmetry, but gaining cubic $Fm\bar{3}m$ symmetry. The appropriate form of gradient energy coefficient for an HCP structure is worked out in two steps to facilitate comparison with the analogous FCC result. We first derive the expression for the contributions to the gradient energy term from the nearest neighbors in the close-packed planes, which are common to both FCC and HCP. This in-plane contribution displays a three-fold sym-

metry, in contrast to the isotropic form which would be expected for a tensor quantity in two dimensions with hexagonal symmetry. We then obtain the full expression for the HCP gradient energy terms by adding the contributions from the six first and six second neighbors in the layers above and below the close-packed plane, which (for the ideal axial ratio of HCP) are at the same distances, but have different arrangements, for the FCC and HCP structures. The resulting HCP model retains the three-fold symmetry in the close-packed planes, as well as isotropic contributions that arise from the second-nearest neighbors.

The HCP model can be used to compute surface energy anisotropies for interphase boundaries (IPBs) between ordered and disorder phases and antiphase boundaries (APBs) between variants of ordered phases. We illustrate the HCP model by giving examples of both IPB and APB interfacial energies as a function of the interface orientation. An analytic solution is possible for a particular type of APB in the A_2B_2 phase, and the closed-form expression for the surface energy exhibits a two-fold axis of symmetry. For IPB boundaries between the disordered and AB_3 ordered phase, a “wetting” of the interface region by the A_2B_2 phase is possible, as in the analogous FCC treatment of Kikuchi and Cahn [5]. In this case the surface energy, computed numerically by integration of the one-dimensional governing equations for a diffuse IPB, exhibits anisotropy that is transverse to the six-fold axis of symmetry. A fourth-rank tensor with hexagonal symmetry would exhibit transverse isotropy [6].

In the following section we describe the discrete model and describe the form of gradient energy coefficient that results from a formal continuum limit of the discrete model. This is followed in Section 3 by application of the model to surface energy calculations for APBs and IPBs. Discussion and conclusions are given in Section 4.

2 Discrete Model

The HCP crystal structure consists of alternating layers of close-packed crystal planes, in which a given atom is surrounded by six neighbors in the basal plane. Three other neighboring atoms appear in each of the close-packed planes immediately above and

below this atom. In HCP these six out-of-plane neighbors are not strictly equivalent to the six in-plane neighbors, but in FCC they are. To facilitate comparison with our FCC results we will at times assume that twelve nearest neighbors surrounding each atom in HCP, as illustrated in Figure 1, are fully equivalent. There is no difference between HCP and FCC in the atomic arrangements of pairs of adjacent close packed planes. In both HCP and FCC there are three first and three second neighbors on each of the adjacent planes.

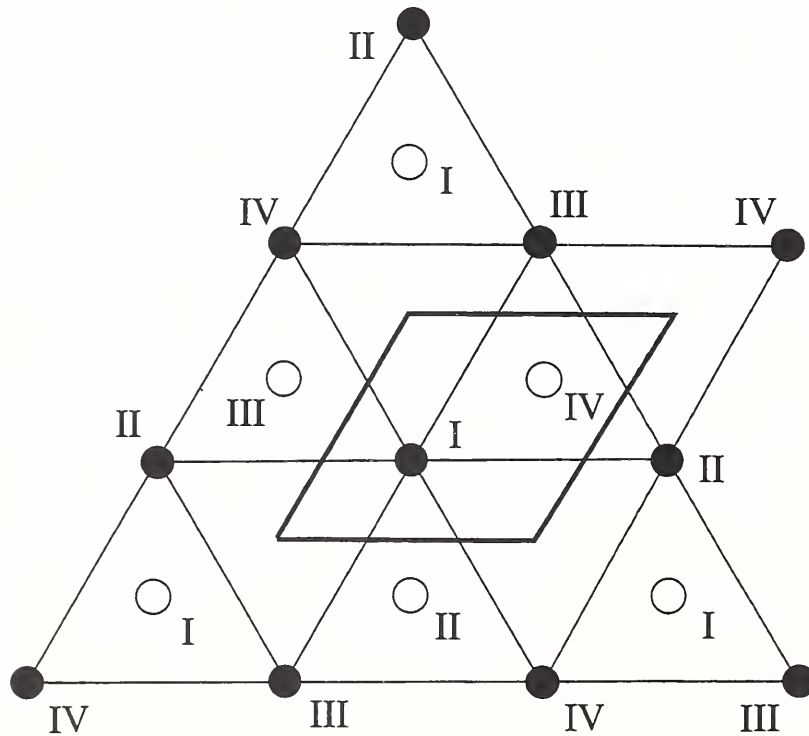


Figure 1. A schematic plot of the hexagonal close packed (HCP) structure, projected onto the basal plane. The labeling of the four distinguished sites for the atomic fractions ρ^I , ρ^{II} , ρ^{III} , and ρ^{IV} in the basal plane (filled symbols) and in the neighboring planes above and below this plane (open circles) is indicated. Also shown by thick lines is the unit cell for the HCP structure. For an ideal axial ratio, the nearest neighbors of the central site labeled I in the figure are the six surrounding neighbors in the basal plane consisting of diametrical pairs of II, III, and IV sites, and the three sites above and the three sites below this plane of types II, III, and IV. The next nearest neighbors are the three sites above and the three sites below this plane that are of type I.

A result of making the twelve neighbors in HCP identical is that there is no difference in the energies, entropies, and free energies of alloys of A and B computed from mean field theories between FCC and HCP if the A-B interactions are the same for first and second neighbor, and there are no longer-range interactions. Consequently there is an exact correspondence to the kinds of ordered phases that form, and the phase diagrams superimpose. Calculations using the cluster variation method find differences in the entropies that lead to changes in the 8th significant figure in the values of the free energy, consistent with estimates from exact expansions [7].

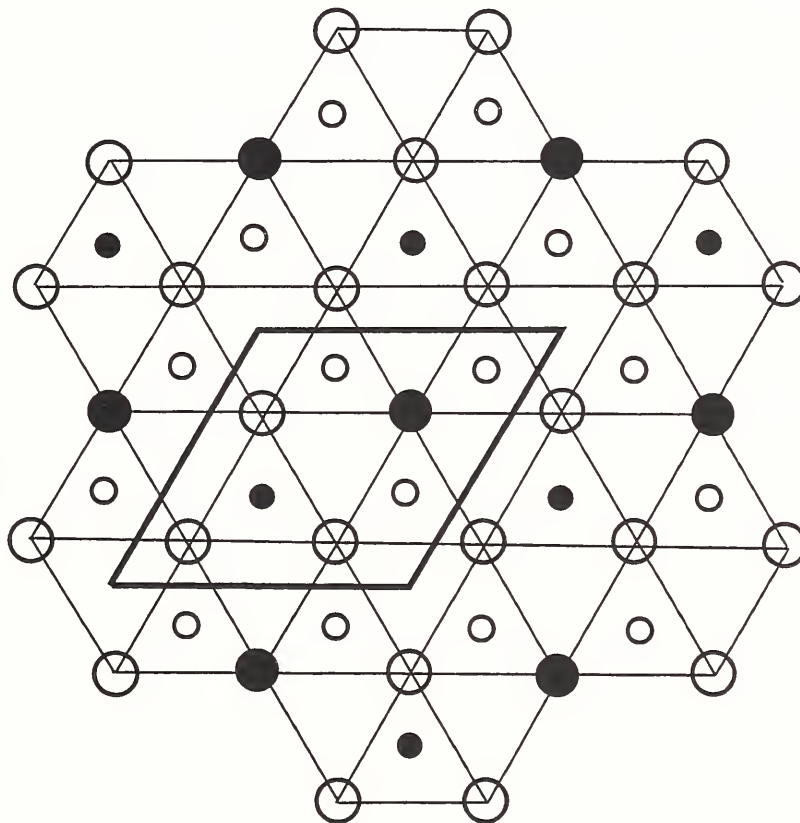


Figure 2. The AB₃ ordered state in an HCP crystal. The filled circles correspond to species A, and the open circles correspond to species B. The larger circles at vertices lie in a basal plane, and the smaller circles at triangle centers lie in the planes above and below this plane. Also shown by the thick lines is the unit cell for the AB₃ ordered structure.

A major distinction between HCP and FCC is that the atoms in an FCC structure occupy the points of an FCC Bravais lattice, whereas in an HCP structure the points of the

hexagonal Bravais lattice are unoccupied. The HCP structure is non-symmorphic; there are no points with the full $6/mmm$ symmetry. The atoms sit on a set of symmetrically equivalent points with symmetry $\bar{6}m2$ that form a lattice complex (a crystallographic orbit, a Wyckoff position), but not a lattice. Another distinction is that the unit cell of FCC is given by three orthogonal lattice vectors \mathbf{a}_i along the cube axes, whereas for the HCP cell there is one vector \mathbf{c} along the six-fold axis and three equivalent but not independent vectors \mathbf{a}_i at 120° . This leads to a four index system (hkil) in which $h+k+i = 0$.

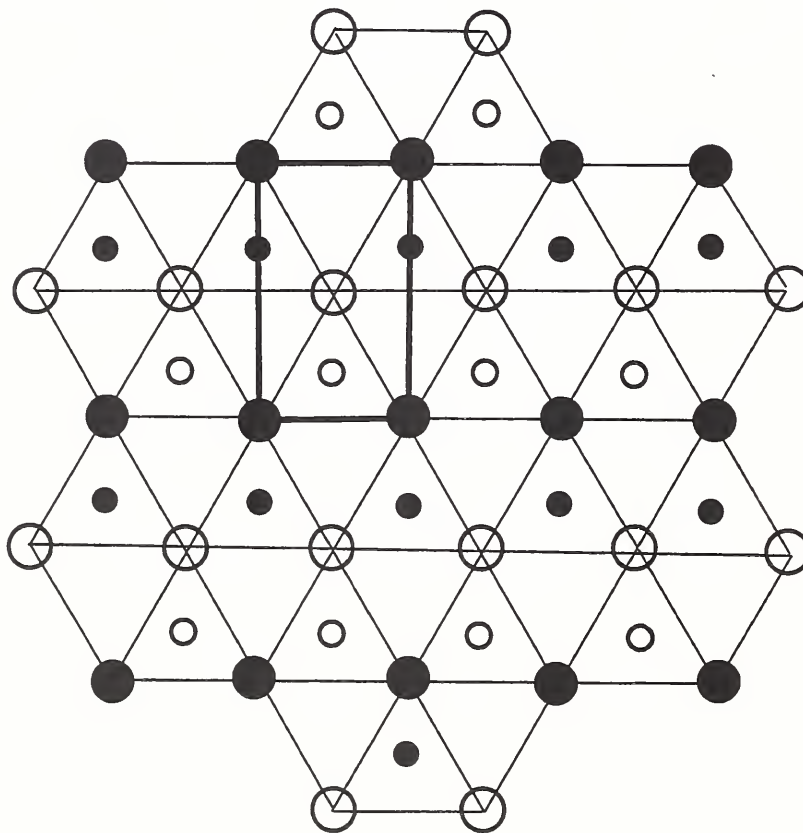


Figure 3. The A_2B_2 ordered state in an HCP crystal (see Figure 2 for a discussion of symbols). Also shown by the thick lines is the unit cell for the A_2B_2 ordered structure.

We will be considering interfaces in a particular ordering of HCP in which the close neighbor interactions would lead to the Cu_3Au and CuAu structures of FCC. A prototype material for these HCP order-disorder transitions is the Cd–Mg system (see, e.g. [8]), which admits the ordered phases Cd_3Mg and CdMg_3 (space group $P6_3mmc$, Strukturbericht designation DO_{19}) near 25 % and 75 % compositions, respectively, and the

CdMg ordered phase (space group $Cmcm$, Strukturbericht designation B_{19}) near 50 % [9]. The Cd_3Mg and CdMg ordered phases are depicted in the next two figures. Figure 2 shows the AB_3 ordering in an HCP crystal structure that describes the Cd_3Mg phase. Figure 3 shows the A_2B_2 ordering that describes the CdMg phase. Our treatment is specifically designed to describe the disordered HCP and ordered Cd_3Mg and CdMg structures in the context of a mean field treatment involving nonconserved order parameters that are smooth, slowly-varying functions of space on the scale of the underlying lattice.

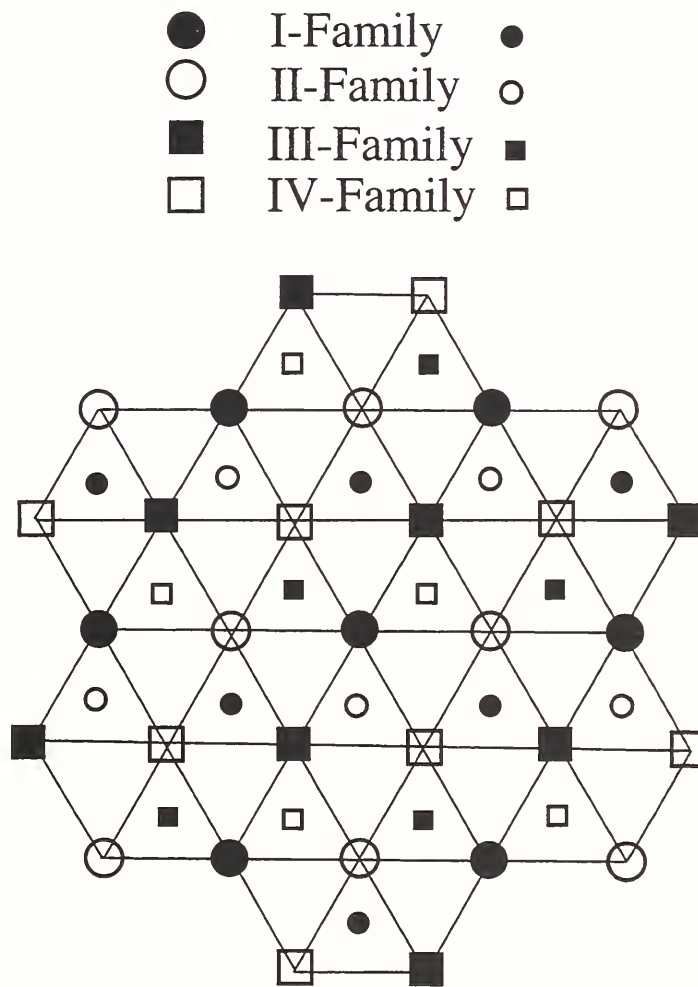


Figure 4. A schematic plot showing an extended portion of the HCP structure denoting the the four independent sites. Larger circles and squares correspond to the in-plane contributions discussed in the text, and the asterisks denote the sites in the neighboring close-packed planes immediately above and below.

Each of these ordered states, as well as the disordered HCP state, can be described with a Nix-Shockley (Bragg-Williams) model having four degrees of freedom, representing the atomic fractions at each of four distinct sites in the structure that is equivalent to what was used for FCC [2]. The labeling of the four families of sites is indicated in Figure 4. Interactions between the A and B atoms in the binary alloy can be characterized by appropriate interaction energies, which we will model approximately by using simple expansions in terms of the local atomic fraction ρ at each site (see, e.g., [10]). Our main concern will be to derive the appropriate form of gradient energy term in a continuum description of the HCP structure, and for this purpose it will suffice to consider nearest and second nearest neighbor interactions that will ultimately determine the form of the free energy functional for the system. With the free energy functional in hand, we are able to compute the surface energy associated with interfaces between different ordered and disorder phases as a function of interface orientation and the other model parameters.

We first discuss the description of the bulk equilibrium states in terms of nonconserved order parameters. To describe inhomogeneous states, such as IPBs and APBs, gradient energy terms are introduced in two stages, first giving the contributions to the free energy that take into account only interactions between atoms in the same plane. We then include the effects arising from out-of-plane interactions to obtain the full expression for the free energy functional that we use to describe the anisotropy of interfacial energy in HCP structures.

2.1 Bulk Equilibrium

The ordered states of the HCP structure that we consider can be characterized in terms of the four parameters ρ^I , ρ^{II} , ρ^{III} , and ρ^{IV} that define the atomic fraction of atom A at each type of site, as shown in Figure 4. These four parameters thus can be viewed as average values of the atomic fraction over these four families. An elementary tetrahedron consisting of one member from each family forms a natural symmetry unit for the structure, and the form of the bulk free energy density must reflect the underlying symmetry associated with relabeling of the indices of the atomic fractions ρ^I , ρ^{II} , ρ^{III} , and ρ^{IV} , which should leave the energy invariant.

As in the treatment by Braun et al. [2], it is convenient to replace the four atomic fractions by a single conserved order parameter that represents the overall atomic fraction of the system, and three nonconserved order parameters that characterize the state of order in the system and for FCC could be identified with the cubic crystal axes. To avoid confusion with Ref. [2], for the HCP crystal we will call these four order parameters respectively $Q_0, Q_1, Q_2,$ and Q_3 . These parameters are defined by

$$Q_0 = \frac{1}{4} \{ \rho^I + \rho^{II} + \rho^{III} + \rho^{IV} \}, \quad (1)$$

$$Q_1 = \frac{1}{4} \{ \rho^I - \rho^{II} + \rho^{III} - \rho^{IV} \}, \quad (2)$$

$$Q_2 = \frac{1}{4} \{ \rho^I + \rho^{II} - \rho^{III} - \rho^{IV} \}, \quad (3)$$

$$Q_3 = \frac{1}{4} \{ \rho^I - \rho^{II} - \rho^{III} + \rho^{IV} \}. \quad (4)$$

Here Q_0 is the average composition and is conserved. A more geometric interpretation of the other nonconserved order parameters $Q_1, Q_2,$ and Q_3 will be given in Section 2.2.1 below when discussing the ordering within a close-packed plane. With this type of model, the disordered state would be indicated by $\rho^I = \rho^{II} = \rho^{III} = \rho^{IV}$, implying that $Q_1 = Q_2 = Q_3 = 0$. Ordered states correspond to non-zero values of any of these three order parameters.

The bulk free energy function, that is, the energy associated with a homogeneous or uniform phase, is assumed to depend on the four atomic fractions $\rho^I, \rho^{II}, \rho^{III},$ and ρ^{IV} , viz $f = f(\rho^I, \rho^{II}, \rho^{III}, \rho^{IV})$, or, equivalently, to depend on $Q_0, Q_1, Q_2,$ and Q_3 , viz $F(Q_i)$. This free energy must take into account the symmetries dictated by the HCP structure. The arguments and resulting form are similar to those for a FCC crystal [2], and we merely summarize the results here. The energy should be invariant to permutations such as

$$\rho^{II} \rightarrow \rho^{III} \rightarrow \rho^{IV}, \quad Q_1 \rightarrow Q_2, Q_2 \rightarrow Q_3, Q_3 \rightarrow Q_1, \quad (5)$$

and to interchanges such as

$$\rho^I \rightarrow \rho^{II}, \rho^{III} \rightarrow \rho^{IV}, \quad Q_1 \rightarrow -Q_1, Q_2 \rightarrow Q_2, Q_3 \rightarrow -Q_3, \quad (6)$$

so that the bulk energy function $F(Q_i)$ must be invariant to permutations in Q_1 , Q_2 , and Q_3 , as well as to sign changes of any two of these variables. Imposing these symmetries leads to an expression of the free energy of the form (see, e.g., Landau and Lifshitz [11])

$$F(Q_i) = a_2(Q_1^2 + Q_2^2 + Q_3^2) + a_3 Q_1 Q_2 Q_3 + a_{41}(Q_1^4 + Q_2^4 + Q_3^4) + a_{42}(Q_1^2 Q_2^2 + Q_2^2 Q_3^2 + Q_3^2 Q_1^2), \quad (7)$$

where we have expressed the free energy as a simple fourth-degree polynomial in Q_1 , Q_2 , and Q_3 with the required symmetry. The coefficients will generally be functions of composition and temperature, but for the purposes of determining the symmetry of gradient energy terms and computing surface energy anisotropy it suffices to assume that the coefficients are constant, with $F = F(Q_1, Q_2, Q_3)$. For example, this would be appropriate for a description of IPBs at a congruent point of the coexistence curves in the phase diagram, where the compositions of the two bulk phases are equal, or for APBs in which negligible concentration variation occurs across the interface.

This free energy function is identical to that used previously in the FCC model of order-disorder transitions [2], and represents the pointwise energy of the site. In our case it allows the description of the disordered HCP phase [with $Q_1 = Q_2 = Q_3 = 0$], the CdMg phase [with $Q_1 = Q_2 = 0$ and $Q_3 \neq 0$, and variants thereof], and the Cd₃Mg phase [with $Q_1 = Q_2 = Q_3 \neq 0$ and variants thereof] that we wish to consider. Inherent limitations of this simplified description are discussed in [2, 12]. The FCC and HCP models differ in the form of the derived gradient energy terms that we consider next.

2.2 Gradient Energy Terms

To describe inhomogeneous states such as IPBs and APBs, we retain the description in terms of the parameters ρ^j or Q_j , but assume that a continuum limit exists in which they are approximated by smooth functions of space that are slowly varying on the scale of the lattice dimensions. The form of the gradient energy terms is then determined by considering the formal limit of a discrete energy as the dimensions of the lattice become small compared to the assumed macroscale lengths.

The point energy $f(\rho)$ and nearest neighbor contributions to the free energy \mathcal{F} of the

discrete system are assumed to have the form

$$\mathcal{F} = \sum_{j,k,l} \left[f(\rho_{j,k,l}) + \frac{\alpha}{2} (\rho_{j+1,k,l} + \rho_{j-1,k,l} + \rho_{j,k+1,l} + \rho_{j,k-1,l} + \rho_{j-1,k+1,l} + \rho_{j+1,k-1,l}) \rho_{j,k,l} \right. \\ \left. + \frac{\alpha'}{2} (\rho_{j,k,l+1} + \rho_{j,k,l-1} + \rho_{j-1,k,l+1} + \rho_{j-1,k,l-1} + \rho_{j,k-1,l+1} + \rho_{j,k-1,l-1}) \rho_{j,k,l} \right], \quad (8)$$

where the indices j and k refer to locations within each close-packed plane as described more fully below, and the index l labels each close-packed plane. Here α and α' represent nearest neighbor interaction energies in the close-packed plane with index l and the neighboring planes with indices $l+1$ and $l-1$, respectively, that are repulsive for positive values of α and α' . For an ideal HCP structure for which all twelve nearest neighbors are equivalent, one would have $\alpha = \alpha'$. The factor of $1/2$ is included to account for the double counting that occurs in the summation over all points. It is convenient to split the summation over l into two sums over even and odd values of l , which each lead to identical contributions in the continuum limit. We therefore focus attention on a representative close-packed plane with index l , and its neighboring close-packed planes above and below with indices $l+1$ and $l-1$.

2.2.1 In-Plane Contribution

If we restrict our attention to the in-plane atomic fractions, a density function for the close-packed plane can be defined in terms of a plane wave expansion as

$$\rho(\vec{x}) = Q_0 + Q_1 \cos \omega \left(\frac{\sqrt{3}}{2}x - \frac{1}{2}y \right) + Q_2 \cos \omega y + Q_3 \cos \omega \left(\frac{\sqrt{3}}{2}x + \frac{1}{2}y \right), \\ = Q_0 + Q_1 \cos \omega y_1 + Q_2 \cos \omega y_2 + Q_3 \cos \omega y_3, \quad (9)$$

where $\omega = 2\pi/(h\sqrt{3})$ is the wavenumber corresponding to the wavelength $\lambda = 2\pi/\omega = \sqrt{3}h$ between the centers of neighboring hexagons. Here h is the edge length of a hexagon. The density function consists of a uniform term proportional to Q_0 , and three terms that represent density variations in each of three directions y_j normal to the three basal lattice vectors \mathbf{a}_j . Specifically, the local coordinates aligned with the lattice vectors are given by $(x_1, y_1) = (-x/2 - \sqrt{3}y/2, \sqrt{3}x/2 - y/2)$, $(x_2, y_2) = (x, y)$, and $(x_3, y_3) =$

$(-x/2 + \sqrt{3}y/2, -\sqrt{3}x/2 - y/2)$. The four atomic fractions are then given in terms of the order parameters by

$$\rho^I = \rho(0, 0) = Q_0 + Q_1 + Q_2 + Q_3, \quad (10)$$

$$\rho^{II} = \rho(h, 0) = Q_0 - Q_1 + Q_2 - Q_3, \quad (11)$$

$$\rho^{III} = \rho(h/2, \sqrt{3}h/2) = Q_0 + Q_1 - Q_2 - Q_3, \quad (12)$$

$$\rho^{IV} = \rho(-h/2, \sqrt{3}h/2) = Q_0 - Q_1 - Q_2 + Q_3. \quad (13)$$

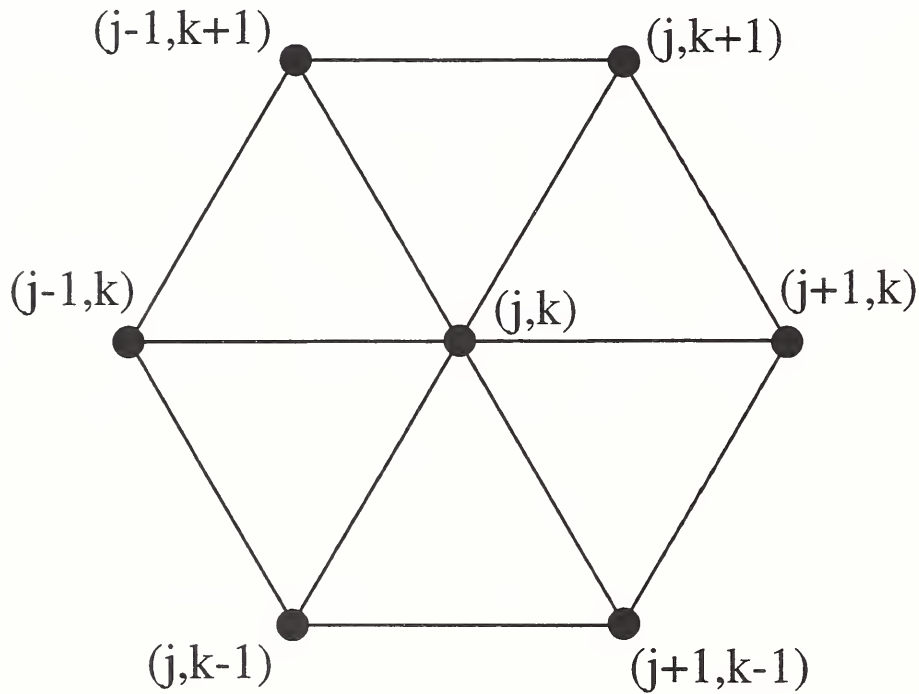


Figure 5. The index notation for the discrete variables prior to passing to a continuum limit.

If the in-plane sites of the HCP crystal are labeled by the coordinates (j, k) as shown in Figure 5, then the in-plane contribution to the energy \mathcal{F}_{IP} from interactions between neighboring in-plane atoms can be written in the form

$$\mathcal{F}_{IP} = \sum_{j,k} \left[f(\rho_{j,k}) + \frac{\alpha}{2} (\rho_{j+1,k} + \rho_{j-1,k} + \rho_{j,k+1} + \rho_{j,k-1} + \rho_{j-1,k+1} + \rho_{j+1,k-1}) \rho_{j,k} \right], \quad (14)$$

as in the Ising model (see, for example, [13]). The sum is rewritten as four sums over each site type,

$$\begin{aligned}
\mathcal{F}_{IP} = & \sum_{\substack{j \text{ even} \\ k \text{ even}}} \left[f(\rho_{j,k}^I) + \frac{\alpha}{2} \left(\rho_{j+1,k}^{II} + \rho_{j-1,k}^{II} + \rho_{j,k+1}^{III} + \rho_{j,k-1}^{III} + \rho_{j-1,k+1}^{IV} + \rho_{j+1,k-1}^{IV} \right) \rho_{j,k}^I \right] \\
& + \sum_{\substack{j \text{ odd} \\ k \text{ even}}} \left[f(\rho_{j,k}^{II}) + \frac{\alpha}{2} \left(\rho_{j+1,k}^I + \rho_{j-1,k}^I + \rho_{j,k+1}^{IV} + \rho_{j,k-1}^{IV} + \rho_{j-1,k+1}^{III} + \rho_{j+1,k-1}^{III} \right) \rho_{j,k}^{II} \right] \\
& + \sum_{\substack{j \text{ even} \\ k \text{ odd}}} \left[f(\rho_{j,k}^{III}) + \frac{\alpha}{2} \left(\rho_{j+1,k}^{IV} + \rho_{j-1,k}^{IV} + \rho_{j,k+1}^I + \rho_{j,k-1}^I + \rho_{j-1,k+1}^{II} + \rho_{j+1,k-1}^{II} \right) \rho_{j,k}^{III} \right] \\
& + \sum_{\substack{j \text{ odd} \\ k \text{ odd}}} \left[f(\rho_{j,k}^{IV}) + \frac{\alpha}{2} \left(\rho_{j+1,k}^{III} + \rho_{j-1,k}^{III} + \rho_{j,k+1}^{II} + \rho_{j,k-1}^{II} + \rho_{j-1,k+1}^I + \rho_{j+1,k-1}^I \right) \rho_{j,k}^{IV} \right]. \quad (15)
\end{aligned}$$

Taylor's Theorem can be applied to the pairwise interactions, giving to leading order the form

$$\begin{aligned}
\mathcal{F}_{IP} = & \sum_{\substack{j \text{ even} \\ k \text{ even}}} \left[\tilde{f}(\rho^I) + \frac{\alpha h^2}{2} \left(\rho_{x_1 x_1}^{III} + \rho_{x_2 x_2}^{II} + \rho_{x_3 x_3}^{IV} \right) \rho^I \right], \\
& + \sum_{\substack{j \text{ odd} \\ k \text{ even}}} \left[\tilde{f}(\rho^{II}) + \frac{\alpha h^2}{2} \left(\rho_{x_1 x_1}^{IV} + \rho_{x_2 x_2}^I + \rho_{x_3 x_3}^{III} \right) \rho^{II} \right], \\
& + \sum_{\substack{j \text{ even} \\ k \text{ odd}}} \left[\tilde{f}(\rho^{III}) + \frac{\alpha h^2}{2} \left(\rho_{x_1 x_1}^I + \rho_{x_2 x_2}^{IV} + \rho_{x_3 x_3}^{II} \right) \rho^{III} \right], \\
& + \sum_{\substack{j \text{ odd} \\ k \text{ odd}}} \left[\tilde{f}(\rho^{IV}) + \frac{\alpha h^2}{2} \left(\rho_{x_1 x_1}^{II} + \rho_{x_2 x_2}^{III} + \rho_{x_3 x_3}^I \right) \rho^{IV} \right], \quad (16)
\end{aligned}$$

where $\tilde{f}(\rho) = f(\rho) + 3\alpha\rho^2$. Here we use subscripts to denote partial derivatives, with $\rho_{x_j}^I = \partial\rho^I/\partial x_j$, and so forth. In the limit $h \rightarrow 0$, the sums over nearest neighbors tend to integrals that, following integration by parts, involve the squares of the derivatives of the atomic fractions.

The resulting expressions can be rewritten in terms of the order parameters Q_j by using the definitions (10)–(13), which leads to gradient energy terms of the form

$$\begin{aligned}
& -\alpha h^2 \left[|\nabla_H Q_1|^2 + |\nabla_H Q_2|^2 + |\nabla_H Q_3|^2 \right] \\
& + 4\alpha h^2 \left\{ \left(\frac{\sqrt{3}}{2} \frac{\partial Q_1}{\partial x} - \frac{1}{2} \frac{\partial Q_1}{\partial y} \right)^2 + \left(\frac{\partial Q_2}{\partial y} \right)^2 + \left(\frac{\sqrt{3}}{2} \frac{\partial Q_3}{\partial x} + \frac{1}{2} \frac{\partial Q_3}{\partial y} \right)^2 \right\} \quad (17) \\
& = -\alpha h^2 \left[|\nabla_H Q_1|^2 + |\nabla_H Q_2|^2 + |\nabla_H Q_3|^2 - 4 \left\{ \left(\frac{\partial Q_1}{\partial y_1} \right)^2 + \left(\frac{\partial Q_2}{\partial y_2} \right)^2 + \left(\frac{\partial Q_3}{\partial y_3} \right)^2 \right\} \right],
\end{aligned}$$

where we have defined $|\nabla_H Q_1|^2 = (\partial Q_1/\partial x)^2 + (\partial Q_1/\partial y)^2$, etc. The terms involving ∇_H have rotation symmetry in the plane, whereas the latter three terms can be shown to have a three-fold symmetry. Since we have assumed that the concentration variation is negligible, no gradients of Q_0 appear in these expressions.

2.2.2 Out-of-plane nearest neighbors

The definition of the sites in the neighboring close-packed plane is shown in Figure 4. The nearest neighbors of ρ^I in the neighboring planes are then ρ^{II} , ρ^{III} , and ρ^{IV} as indicated. The vertical distance between close-packed planes for the ideal axial ratio is given by $\sqrt{6}h/3$.

In this case a typical out-of-plane interaction term has the form

$$\rho^I(0, 0, 0) \rho^{II}(0, -h/\sqrt{3}, \pm\sqrt{6}h/3), \quad (18)$$

$$\rho^I(0, 0, 0) \rho^{III}(-h/2, h/2\sqrt{3}, \pm\sqrt{6}h/3), \quad (19)$$

or

$$\rho^I(0, 0, 0) \rho^{IV}(h/2, h/2\sqrt{3}, \pm\sqrt{6}h/3). \quad (20)$$

Permutations of these expressions result from the contributions centered at the sites II , III , and IV . Taking into account all the symmetries, and evaluating in a similar

method to the in-plane nearest neighbors, the contributions from the out-of-plane nearest neighbors take the form

$$\alpha' h^2 \left[|\nabla_H Q_1|^2 + |\nabla_H Q_2|^2 + |\nabla_H Q_3|^2 - \frac{4}{3} \left\{ \left(\frac{\partial Q_1}{\partial y_1} \right)^2 + \left(\frac{\partial Q_2}{\partial y_2} \right)^2 + \left(\frac{\partial Q_3}{\partial y_3} \right)^2 \right\} + \frac{4}{3} \left\{ \left(\frac{\partial Q_1}{\partial z} \right)^2 + \left(\frac{\partial Q_2}{\partial z} \right)^2 + \left(\frac{\partial Q_3}{\partial z} \right)^2 \right\} \right]. \quad (21)$$

Setting $\alpha' = \alpha$ makes the in-plane and out-of-plane interactions equal.

2.2.3 Full Expression for Nearest Neighbor Interactions

When $\alpha' = \alpha$ adding together the in-plane and out-of-plane contributions gives the expression

$$\frac{4\alpha h^2}{3} \left\{ 2 \left(\frac{\sqrt{3}}{2} \frac{\partial Q_1}{\partial x} - \frac{1}{2} \frac{\partial Q_1}{\partial y} \right)^2 + 2 \left(\frac{\partial Q_2}{\partial y} \right)^2 + 2 \left(\frac{\sqrt{3}}{2} \frac{\partial Q_3}{\partial x} + \frac{1}{2} \frac{\partial Q_3}{\partial y} \right)^2 + \left(\frac{\partial Q_1}{\partial z} \right)^2 + \left(\frac{\partial Q_2}{\partial z} \right)^2 + \left(\frac{\partial Q_3}{\partial z} \right)^2 \right\}. \quad (22)$$

Note that the dependence on the z derivatives in this expression is much simpler than those for x and y derivatives, which show the three-fold symmetry mentioned previously. The x and y derivatives in the free energy define directional derivatives in the directions normal to the symmetry planes of the hexagons, in a manner reminiscent of the form for the density $\rho(\vec{x})$ given in Eq. (9).

2.2.4 Second-Nearest-Neighbors

We will also include gradient energy contributions arising from second nearest neighbor interactions, which will be assumed to be attractive. Referring to Figure 1, the second nearest neighbors of a given site are of the same family, located in the planes immediately above and below the site. Similar methods were applied to the second nearest neighbors, and the results are isotropic:

$$|\nabla \rho^I|^2 + |\nabla \rho^{II}|^2 + |\nabla \rho^{III}|^2 + |\nabla \rho^{IV}|^2 \sim |\nabla Q_1|^2 + |\nabla Q_2|^2 + |\nabla Q_3|^2, \quad (23)$$

where $|\nabla Q_1|^2 = |\nabla_H Q_1|^2 + (\partial Q_1/\partial z)^2$, etc. This result is similar to that found for the FCC model [2], where the effects of the second nearest neighbor interactions was also found to be isotropic.

2.3 Governing Equations

When $\alpha' = \alpha$ the continuum free energy functional, including nearest and second-nearest neighbor interactions and the bulk energy, thus has the form

$$\mathcal{F} = \int \left\{ F(Q_1, Q_2, Q_3) + \frac{A}{2} \left[2 \left(\frac{\sqrt{3}}{2} \frac{\partial Q_1}{\partial x} - \frac{1}{2} \frac{\partial Q_1}{\partial y} \right)^2 + 2 \left(\frac{\partial Q_2}{\partial y} \right)^2 + 2 \left(\frac{\sqrt{3}}{2} \frac{\partial Q_3}{\partial x} + \frac{1}{2} \frac{\partial Q_3}{\partial y} \right)^2 + \left(\frac{\partial Q_1}{\partial z} \right)^2 + \left(\frac{\partial Q_2}{\partial z} \right)^2 + \left(\frac{\partial Q_3}{\partial z} \right)^2 \right] + \frac{B}{2} [|\nabla Q_1|^2 + |\nabla Q_2|^2 + |\nabla Q_3|^2] \right\} dV. \quad (24)$$

Here A and B are positive constants that are proportional to the nearest and second nearest neighbor interaction energies, respectively. When $\alpha' \neq \alpha$ the $(\partial Q_1/\partial z)^2 + (\partial Q_2/\partial z)^2 + (\partial Q_3/\partial z)^2$ term will be multiplied by a third independent positive constant.

The steady-state governing equations for equilibrium solutions take the form

$$0 = \frac{\delta \mathcal{F}}{\delta Q_1} = \frac{\partial F}{\partial Q_1} - B \nabla^2 Q_1 - A \left(\frac{\partial^2 Q_1}{\partial z^2} + 2 \left[\frac{3}{4} \frac{\partial^2 Q_1}{\partial x^2} - \frac{\sqrt{3}}{2} \frac{\partial^2 Q_1}{\partial x \partial y} + \frac{1}{4} \frac{\partial^2 Q_1}{\partial y^2} \right] \right), \quad (25)$$

$$0 = \frac{\delta \mathcal{F}}{\delta Q_2} = \frac{\partial F}{\partial Q_2} - B \nabla^2 Q_2 - A \left(\frac{\partial^2 Q_2}{\partial z^2} + 2 \frac{\partial^2 Q_2}{\partial y^2} \right), \quad (26)$$

$$0 = \frac{\delta \mathcal{F}}{\delta Q_3} = \frac{\partial F}{\partial Q_3} - B \nabla^2 Q_3 - A \left(\frac{\partial^2 Q_3}{\partial z^2} + 2 \left[\frac{3}{4} \frac{\partial^2 Q_3}{\partial x^2} + \frac{\sqrt{3}}{2} \frac{\partial^2 Q_3}{\partial x \partial y} + \frac{1}{4} \frac{\partial^2 Q_3}{\partial y^2} \right] \right). \quad (27)$$

This expression allows the prediction of the dependence of surface energy between two bulk phases on the orientation of the interface, as we will next discuss.

2.3.1 Surface Energy

An IPB between the disordered HCP phase and an ordered phase can exist when the free energy densities of the two bulk phases are equal. In general a common tangent construction relates the bulk compositions on either side of the interface, but in our approximate treatment such variations in composition are neglected. To define the surface energy, consider a one-dimensional solution that depends on a single variable, $\zeta = \mathbf{x} \cdot \hat{\mathbf{n}}$,

which varies in the direction of a given unit vector $\hat{\mathbf{n}}$. The partial derivatives of the order parameters Q_j then have the form $\partial Q_j / \partial x_k = n_k dQ_j / d\zeta$. The second nearest neighbor interactions are isotropic, since $|\nabla Q_j|^2 = (dQ_j / d\zeta)^2$, with no dependence on $\hat{\mathbf{n}}$. The surface energy, γ , is defined in terms of the free energy per unit area:

$$\gamma = \frac{\mathcal{F}}{\mathcal{A}} = \int \left\{ \frac{\xi_1}{2} \left(\frac{dQ_1}{d\zeta} \right)^2 + \frac{\xi_2}{2} \left(\frac{dQ_2}{d\zeta} \right)^2 + \frac{\xi_3}{2} \left(\frac{dQ_3}{d\zeta} \right)^2 + F(Q_1, Q_2, Q_3) \right\} d\zeta, \quad (28)$$

where the orientation-dependent coefficients ξ_j are

$$\xi_1 = A \left[2 \left(\frac{\sqrt{3}}{2} n_x - \frac{1}{2} n_y \right)^2 + n_z^2 \right] + B, \quad (29)$$

$$\xi_2 = A [2n_y^2 + n_z^2] + B, \quad (30)$$

$$\xi_3 = A \left[2 \left(\frac{\sqrt{3}}{2} n_x + \frac{1}{2} n_y \right)^2 + n_z^2 \right] + B. \quad (31)$$

(Note from (7) that $F(0, 0, 0) = 0$).

The governing equations that describe two equilibrium phases in contact can then be computed by taking the variation of either the full energy functional (24), which results in a partial differential equation, or the above surface energy functional. The latter results in ordinary differential equations that have the form

$$\xi_1 \frac{d^2 Q_1}{d\zeta^2} = \frac{\partial F}{\partial Q_1}, \quad (32)$$

$$\xi_2 \frac{d^2 Q_2}{d\zeta^2} = \frac{\partial F}{\partial Q_2}, \quad (33)$$

$$\xi_3 \frac{d^2 Q_3}{d\zeta^2} = \frac{\partial F}{\partial Q_3}, \quad (34)$$

These equations are to be applied over the range $-\infty < \zeta < \infty$, with far-field values given by the bulk equilibrium values in each phase. The equations admit the first integral

$$\frac{\xi_1}{2} \left(\frac{dQ_1}{d\zeta} \right)^2 + \frac{\xi_2}{2} \left(\frac{dQ_2}{d\zeta} \right)^2 + \frac{\xi_3}{2} \left(\frac{dQ_3}{d\zeta} \right)^2 = F(Q_1, Q_2, Q_3) + \text{constant}, \quad (35)$$

which allows explicit evaluation of the surface energy in special cases.

3 Results

We give two examples of surface energy computations using the model. The first uses a closed form solution representing an interface between two variants of the same phase for the A_2B_2 state. The second uses a numerical solution to compute the surface energy of an interface between the disordered HCP phase and the ordered AB_3 phase.

3.1 Anti-Phase Boundary

An analytic solution can be obtained for a special case of an anti-phase boundary (APB) between two variants of the same phase. We consider domains with the ordered structure A_2B_2 , characterized by a single non-zero order parameter, $Q_2 \neq 0$. The relations between the order parameters and site densities then give

$$\rho^I = Q_0 + Q_2, \quad (36)$$

$$\rho^{II} = Q_0 + Q_2, \quad (37)$$

$$\rho^{III} = Q_0 - Q_2, \quad (38)$$

$$\rho^{IV} = Q_0 - Q_2. \quad (39)$$

For a stoichiometric composition $Q_0 = 1/2$ appropriate to the A_2B_2 phase, the atomic fractions $\rho^I = \rho^{II} = 1$ and $\rho^{III} = \rho^{IV} = 0$ correspond to the value $Q_2 = 1/2$, i.e., site I and II have A atoms and sites III and IV have B atoms. The choice $Q_0 = 1/2$ and $Q_2 = -1/2$ leads to $\rho^I = \rho^{II} = 0$ and $\rho^{III} = \rho^{IV} = 1$, reversing the occupation pattern. The two states with $Q_0 = 1/2$ and $Q_2 = \pm 1/2$ are identical up to a shift by $\sqrt{3}h/2$ in the y -direction.

For $Q_1 = Q_3 = 0$, the governing equations reduce to a single second order equation for Q_2 that has the solution

$$Q_2(\zeta) = \frac{1}{2} \tanh\left(\frac{\zeta}{2\zeta_0}\right), \quad (40)$$

for $-a_2 = a_{41}/2 > 0$, where ζ_0 is a characteristic interface width given by $\zeta_0^2 = \xi_2/(2a_{41})$.

The surface energy can then be evaluated explicitly to give

$$\gamma = \frac{\sqrt{2a_{41}\xi_2}}{6} \sqrt{A(1 - n_x^2 + n_y^2) + B} = \frac{\sqrt{2a_{41}\xi_2}}{6} \sqrt{A(1 - \sin^2\theta \cos 2\phi) + B}, \quad (41)$$

where we have written the normal vector in spherical angles as $\hat{\mathbf{n}} = (\sin \theta \cos \phi, \sin \theta \sin \phi, \cos \theta)$, For $A = 0$ and $B \neq 0$, the surface energy is isotropic (independent of $\hat{\mathbf{n}}$). The strongest anisotropy is obtained if $A \neq 0$ and $B = 0$. In this case, the energy of a surface with normal $\hat{\mathbf{n}} = (1, 0, 0)$ vanishes, whereas the surface energy is highest for a surface with normal $\hat{\mathbf{n}} = (0, 1, 0)$. Figure 6 shows a contour plot of the function $\gamma(\phi, \theta)$, corresponding to the case $A = 0.95$ and $B = 0.05$. For these values the ratio of minimum to maximum surface energy is given by $\gamma_{\min}/\gamma_{\max} = 0.16$. The surface energy has a saddle point in the direction $\hat{\mathbf{n}} = (0, 0, 1)$, and Figure 6 has a two-fold axis of symmetry about this direction. The equatorial plane is also a plane of symmetry. The overall symmetry is mmm.

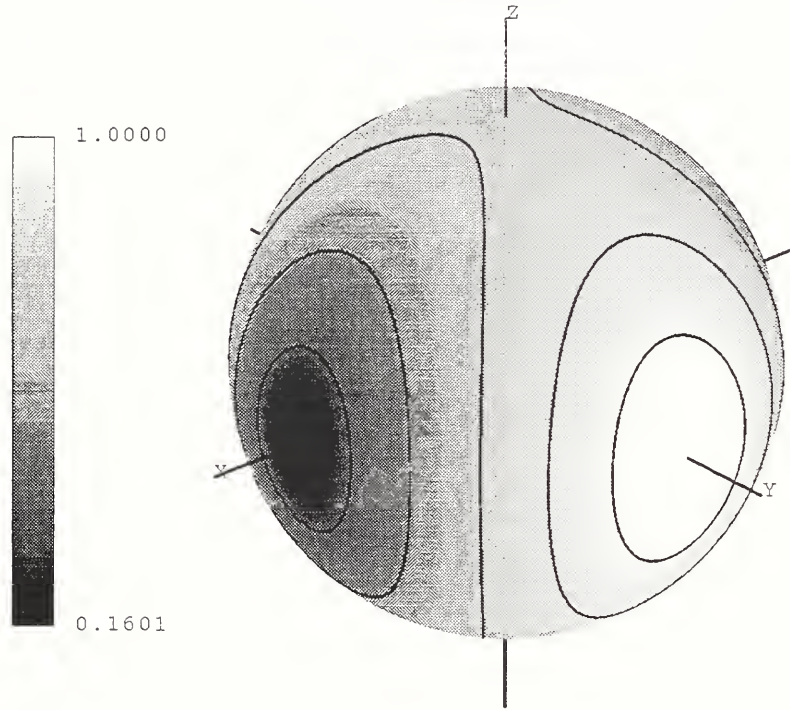


Figure 6. Contour plots of the HCP- A_2B_2 APB surface energy $\gamma(\phi, \theta)$. The surface energy has two minima and two maxima along the equator of the sphere.

3.2 Interphase-Phase Boundary

We next consider the case of an inter-phase boundary (IPB) connecting the disordered HCP phase with $Q_1 = Q_2 = Q_3 = 0$ with the ordered AB_3 phase. At the composition $Q_0 = 1/4$, the ordered phase can be represented by atomic fractions $\rho^I = 1$ and $\rho^{II} = \rho^{III} = \rho^{IV} = 0$, corresponding to the order parameter values $Q_1 = Q_2 = Q_3 = 1/4$.

An analytic solution is possible for an IPB with $\hat{n} = (0, 0, 1)$, in which case $\xi_1 = \xi_2 = \xi_3 = (A+B)$. For an IPB to exist the coefficients are related by $(a_{41} + a_{42}) = 4a_2 > 0$ and $a_3 = -24a_2$; these relations effectively define the HCP- AB_3 congruent temperature in our model. The governing equations then admit a solution with $Q_1 = Q_2 = Q_3$ throughout the IPB, and the solution is given by

$$Q_1(\zeta) = \frac{1}{8} \left[1 + \tanh \left(\frac{\zeta}{\zeta_1} \right) \right], \quad (42)$$

where $\zeta_1^2 = 2\xi_1/(3a_2)$, with surface energy $\gamma = \sqrt{6\xi_1 a_2}/96$.

For $\hat{n} = (1, 0, 0)$ we have $\xi_1 = \xi_3 = (3A/2 + B)$ and $\xi_2 = B$. A solution with $Q_1 = Q_3$ is possible, and the governing equations take the form

$$\left(\frac{3}{2}A + B \right) \frac{d^2 Q_1}{d\zeta^2} = \frac{\partial F}{\partial Q_1}(Q_1, Q_2, Q_1), \quad (43)$$

$$B \frac{d^2 Q_2}{d\zeta^2} = \frac{\partial F}{\partial Q_2}(Q_1, Q_2, Q_1). \quad (44)$$

This case is identical to that considered by Braun et al. [2] for a [001] Cu_3Au IPB, the FCC Cu_3Au phase being the analog of the HCP Cd_3Mg phase. As shown in [2], in the limit that $B/A \ll 1$, the IPB has an interior layer where Q_2 becomes small compared to Q_1 , which represents ‘‘wetting’’ by the $CdMg$ phase. Surprisingly, this can occur even under conditions for which $CdMg$ does not exist as a bulk phase. It is possible to derive asymptotic expansions that describe the solution for $B/A \ll 1$; see [2] for details.

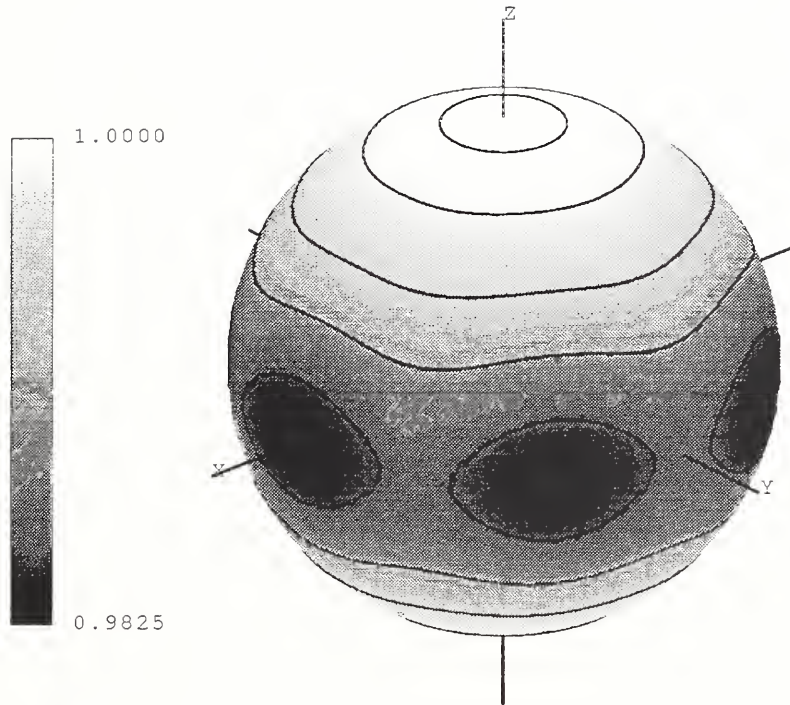


Figure 7. Contour plots of the HCP-AB₃ IPB surface energy $\gamma(\phi, \theta)$. The IPB surface energy has six minima evenly spaced along the equator and maxima at the poles.

For general orientations analytical solutions are not known, and we have computed numerical solutions to the governing equations by using the program COLSYS [14] (see [2]). Results are shown in Figure 7, where contours of the surface energy $\gamma(\phi, \theta)$ are shown, again corresponding to the case $A = 0.95$ and $B = 0.05$. In this case the surface energy anisotropy is much milder than in the previous case of an APB, with $\gamma_{\min}/\gamma_{\max} = 0.98$. The symmetry of the energy is also different. The IPB surface energy has a six-fold axis of symmetry about the orientation $\hat{\mathbf{n}} = (0, 0, 1)$, which is the orientation of maximum energy. The energy is a minimum for the orientation $\hat{\mathbf{n}} = (1, 0, 0)$.

4 Conclusion

The model developed in this paper obtains a gradient energy theory for anisotropic interfaces between ordered and disorder phases from a discrete Bragg-Williams formulation. The result of analytical and numerical solutions of nonlinear ordinary differential equations is a prediction of the dependence of surface free energy on the orientation for anti-phase boundary and inter-phase boundary models. In all cases, the orientation dependence that is found is consistent with the symmetry of the problem; in particular, for the APB associated by a shift between two parallel domains of the CdMg structure, the anisotropy expected and found was orthorhombic and quite strong.

For discrete theories of interfaces the anisotropy conforms to the crystallographic symmetry. In going to a continuum gradient theory additional symmetries appear. Thus for a scalar order parameter, gradient energy coefficients correspond to a tensor of rank two, and would be completely isotropic for an interface between two aligned cubic phases. For hexagonal crystals this tensor can be represented by a matrix with two parameters. This gives a simple axial anisotropy but no transverse one. For the multiple order parameter model considered here, the HCP gradient energy coefficients c_{ijkl} that appear in the gradient energy term in Eq. (24) depend on two parameters, and the resulting surface energy of an interface between two aligned hexagonal phases, such as the IPB we calculate in this paper, do not have transverse isotropy in the plane but exhibits six-fold symmetry. By contrast, the elastic tensor for an hexagonal crystal contains five parameters and is isotropic in the basal plane [6].

In both this work and in related work for an FCC alloy [2], we have considered multiple order parameter models with gradient energy terms that are quadratic in the spatial derivatives of the order parameters. The multiple order parameters we used in both the FCC and HCP models have a crystallographic character, but the three order parameters that are used in each case do not constitute components of a vector (tensor of rank one), and strictly speaking these are “multiple order parameter models” but not “vector order parameter models.”

For the FCC model the three order parameters could be considered amplitudes of

plane waves aligned with the crystallographic axes, but under changes of axis that preserve cubic symmetry the components do not transform like a vector [2]. The gradient energy contribution can be compared with an analogous expression based on the gradients of vector quantity rather than gradients of the FCC order parameters. If the energy associated with the vector gradient is expressed as a quadratic form the coefficients form a fourth rank tensor which must conform to the symmetry of the crystal. The vector gradient need not be symmetric and can be expressed as a sum of a symmetric and antisymmetric tensors. In a crystal with cubic symmetry no more than three independent coefficients can occur for the energy due to the symmetric part, which in elasticity would be termed C_{11} , C_{12} , and C_{44} , while a fourth coefficient may be needed for the energy due to the antisymmetric part [15]. The FCC gradient energy coefficients are analogous to a restricted form of the tensor case: of the three possible coefficients for the symmetric part, the one corresponding to C_{12} vanishes, while the coefficient corresponding to the antisymmetric part is identical to C_{44} . This is a minor difference, and the anisotropy is consistent with that of a vector order parameter model with two additional restrictions on the coefficients.

For the HCP model, in the basal plane the three order parameters appear as composition waves aligned with the three hexagonal axes \mathbf{a}_j , which are in the plane and thus not independent. In three dimensions, because of the non-symmorphic character of the structure, the order parameters are not easily identified with plane waves. Since the HCP order parameters do not transform as a vector, the associated coefficients c_{ijkl} that appear in the gradient energy term in Eq. (24) do not have the transformation properties of a tensor of rank four under changes of coordinates. The different symmetries associated with the order parameters and the spatial coordinates are apparent in the form of the energy functional in Eq. (24): the three order parameters Q_j appear symmetrically, whereas the z -axis is distinguished in this expression. For an HCP structure with the ideal axial ratio ($\alpha' = \alpha$), the gradient energy has two coefficients, as in our cubic calculations. Had we imposed that $\alpha' \neq \alpha$ there would have been three parameters. In either case there is a term which is not isotropic transverse to the z axis. Its consequences can be seen in the results for the IPB free energies, which display a distinct six-fold anisotropy.

A multiple order parameter of the kind that we have used here and in the previous papers leads naturally to anisotropy in a continuum model. Anisotropy has been introduced artificially in calculations with a scalar order parameter by making the gradient energy coefficients depend on the direction of the gradient [16]. Any surface energy anisotropy can be modeled in this way, but it cannot be deduced from a physical model. In addition, for a constant mobility the kinetic anisotropy is directly proportional to the interfacial anisotropy. In our FCC work we found that kinetic anisotropies naturally derived from this multiple order parameter model were far greater than the surface energy anisotropies; quite mild energy anisotropies led to nonconvex kinetic anisotropies and sharp corners [3]. We have not explored the full range of anisotropies that are accessible for the HCP model, but we expect nonconvex growth behavior, maybe even six-fold structures analogous to snow flakes, without resorting to the addition of an artificial anisotropy.

5 Acknowledgments

The authors are grateful to R.J. Braun for providing advice on converting the original numerical routine developed for FCC models to the HCP model considered here. This research was partially supported by the Microgravity Research Division of NASA.

Appendix

The expression (17) for the in-plane nearest neighbor interactions can be used to rederive the form of the gradient energy term for FCC crystal structure [2] by combining it with a modified out-of-plane contribution that accounts for the difference in arrangement of the neighboring layers in FCC and HCP structures.

The near-neighbor contributions to the FCC gradient energy term have the simple form

$$\left(\frac{\partial Q_3}{\partial x'}\right)^2 + \left(\frac{\partial Q_1}{\partial y'}\right)^2 + \left(\frac{\partial Q_2}{\partial z'}\right)^2 \quad (45)$$

where the primed variables refer to the coordinates used in Ref. [2], where the coordinate system is aligned with the cube axes of the FCC crystal. The definitions of the order

parameters in Eq. (45) are consistent with our usage in this paper, but differ from those used in Ref. [2] by a permutation given by $Q_3 \rightarrow X$, $Q_1 \rightarrow Y$, and $Q_2 \rightarrow Z$ due the different labeling of the densities. The z axis is the [111] direction in the (x', y', z') system, and the primed coordinates are related to the coordinates used in this paper by the rotation matrix

$$\begin{pmatrix} x' \\ y' \\ z' \end{pmatrix} = \begin{pmatrix} -1/\sqrt{2} & -1/\sqrt{6} & 1/\sqrt{3} \\ 1/\sqrt{2} & -1/\sqrt{6} & 1/\sqrt{3} \\ 0 & \sqrt{2}/\sqrt{3} & 1/\sqrt{3} \end{pmatrix} \begin{pmatrix} x \\ y \\ z \end{pmatrix}. \quad (46)$$

In the (x, y, z) coordinate system, a typical out-of-plane interaction term for FCC has the form

$$\rho^I(0, 0, 0) \rho^{II}(0, \mp h/\sqrt{3}, \pm\sqrt{6}h/3), \quad (47)$$

$$\rho^I(0, 0, 0) \rho^{III}(-h/2, \pm h/2\sqrt{3}, \pm\sqrt{6}h/3), \quad (48)$$

or

$$\rho^I(0, 0, 0) \rho^{IV}(h/2, \pm h/2\sqrt{3}, \pm\sqrt{6}h/3). \quad (49)$$

in which similar families above and below the close-packed plane are reflections of one another through the center of symmetry, rather than mirror reflections through the plane as in the HCP packing.

The resulting contribution from the out-of-plane nearest neighbors can be written in the form

$$\begin{aligned} & \frac{\alpha h^2}{2} \left\{ \frac{8}{3} \left[\left(\frac{\partial Q_1}{\partial z} \right)^2 + \left(\frac{\partial Q_2}{\partial z} \right)^2 + \left(\frac{\partial Q_3}{\partial z} \right)^2 \right] + 8\sqrt{\frac{2}{3}} \left[\frac{\partial Q_1}{\partial x} \frac{\partial Q_1}{\partial z} - \frac{\partial Q_3}{\partial x} \frac{\partial Q_3}{\partial z} \right] \right. \\ & \quad + 8\frac{\sqrt{2}}{3} \left[-\frac{\partial Q_1}{\partial y} \frac{\partial Q_1}{\partial z} + 2\frac{\partial Q_2}{\partial y} \frac{\partial Q_2}{\partial z} - \frac{\partial Q_3}{\partial y} \frac{\partial Q_3}{\partial z} \right] + 2 \left(\frac{\partial Q_2}{\partial x} \right)^2 \\ & \quad \left. + \frac{2}{3} \left[2 \left(\frac{\partial Q_1}{\partial y} \right)^2 - \left(\frac{\partial Q_2}{\partial y} \right)^2 + 2 \left(\frac{\partial Q_3}{\partial y} \right)^2 \right] + \frac{4}{\sqrt{3}} \left[\frac{\partial Q_1}{\partial x} \frac{\partial Q_1}{\partial y} - \frac{\partial Q_3}{\partial x} \frac{\partial Q_3}{\partial y} \right] \right\}, \quad (50) \end{aligned}$$

which factors to give

$$4\alpha h^2 \left\{ \left[\frac{-1}{\sqrt{2}} \frac{\partial Q_3}{\partial x} - \frac{1}{\sqrt{6}} \frac{\partial Q_3}{\partial y} + \frac{1}{\sqrt{3}} \frac{\partial Q_3}{\partial z} \right]^2 + \left[\frac{1}{\sqrt{2}} \frac{\partial Q_1}{\partial x} - \frac{1}{\sqrt{6}} \frac{\partial Q_1}{\partial y} + \frac{1}{\sqrt{3}} \frac{\partial Q_1}{\partial z} \right]^2 \right\}$$

$$\begin{aligned}
& + \left[\sqrt{\frac{2}{3}} \frac{\partial Q_2}{\partial y} + \frac{1}{\sqrt{3}} \frac{\partial Q_2}{\partial z} \right]^2 \Big\} + \alpha h^2 \left[|\nabla_H Q_1|^2 + |\nabla_H Q_2|^2 + |\nabla_H Q_3|^2 \right] \quad (51) \\
& - 4\alpha h^2 \left\{ \left(\frac{\sqrt{3}}{2} \frac{\partial Q_1}{\partial x} - \frac{1}{2} \frac{\partial Q_1}{\partial y} \right)^2 + \left(\frac{\partial Q_2}{\partial y} \right)^2 + \left(\frac{\sqrt{3}}{2} \frac{\partial Q_3}{\partial x} + \frac{1}{2} \frac{\partial Q_3}{\partial y} \right)^2 \right\}.
\end{aligned}$$

Adding the in-plane contribution (17) to the out-of-plane contribution (51) recovers the full expression for the nearest neighbor contributions to the FCC gradient energy term,

$$\begin{aligned}
& 4\alpha h^2 \left\{ \left[\frac{-1}{\sqrt{2}} \frac{\partial Q_3}{\partial x} - \frac{1}{\sqrt{6}} \frac{\partial Q_3}{\partial y} + \frac{1}{\sqrt{3}} \frac{\partial Q_3}{\partial z} \right]^2 + \left[\frac{1}{\sqrt{2}} \frac{\partial Q_1}{\partial x} - \frac{1}{\sqrt{6}} \frac{\partial Q_1}{\partial y} + \frac{1}{\sqrt{3}} \frac{\partial Q_1}{\partial z} \right]^2 \right. \\
& \left. + \left[\sqrt{\frac{2}{3}} \frac{\partial Q_2}{\partial y} + \frac{1}{\sqrt{3}} \frac{\partial Q_2}{\partial z} \right]^2 \right\} = 4\alpha h^2 \left\{ \left(\frac{\partial Q_3}{\partial x'} \right)^2 + \left(\frac{\partial Q_1}{\partial y'} \right)^2 + \left(\frac{\partial Q_2}{\partial z'} \right)^2 \right\}, \quad (52)
\end{aligned}$$

where we have used the coordinate transformation (46) to simplify the final expression.

References

- [1] J. W. Cahn and J. E. Hilliard, Free energy of a nonuniform system. I. Interfacial free energy, *J. Chem. Phys.* **28**:258–267 (1958).
- [2] R. J. Braun, J. W. Cahn, G. B. McFadden, and A. A. Wheeler, Anisotropy of interfaces in an ordered alloy: a multiple-order-parameter model, *Phil. Trans. Roy. Soc. London A* **355**:1787–1833 (1997).
- [3] R. J. Braun, J. W. Cahn, G. B. McFadden, H.E. Rushmeier, and A. A. Wheeler, Theory of anisotropic growth rates in the ordering of an F.C.C. alloy, *Acta Mater.* **46**:1–12 (1998).
- [4] J. F. Nye, *Physical properties of crystals* (Clarendon, Oxford, 1985).
- [5] R. Kikuchi and J. W. Cahn, Theory of interphase and antiphase boundaries in FCC alloys, *Acta Metall.* **27**:1337–1353 (1979).
- [6] A. E. H. Love, *A Treatise on the Mathematical Theory of Elasticity*, (Dover, New York, 1944), pp. 159–161.

- [7] P. Cenedese and J. W. Cahn, Ordering in Close-Packed Structures: A Comparison of HCP and FCC using CVM, *Progr. Theo. Physics*, Supplement **115**:95-113 (1994).
- [8] *Metals Handbook*, 10th ed. (The American Society for Metals, Cleveland, 1990), p. 666.
- [9] F. Ducastelle, *Order and Phase Stability in Alloys* (North Holland, Amsterdam, 1991).
- [10] C. Kittel, *Introduction to Solid State Physics* (Wiley, New York, 1965), p. 337 ff.
- [11] L. D. Landau and E. M. Lifshitz, *Statistical Physics* (Pergammon, London, 1958), Chapter 14.
- [12] R. J. Braun, J. Zhang, J. W. Cahn, G. B. McFadden, and A. A. Wheeler, Multiple-Order-Parameter Theory with a Model Phase Diagram for an fcc Alloy, in preparation.
- [13] K. Huang, *Statistical Mechanics* (Wiley, New York, 1963).
- [14] G. Bader and U. Ascher, *SIAM J. Sci. Stat. Comput.* **8**:483–500 (1987).
- [15] J. W. Cahn and G. B. McFadden, unpublished research.
- [16] G. B. McFadden, A. A. Wheeler, R. J. Braun, S. R. Coriell, and R. F. Sekerka, Phase-field models for anisotropic interfaces, *Phys. Rev. E* **48**:2016–2024 (1993).

